ORIGINAL ARTICLE

Cell surface integrin α5ß1 clustering negatively regulates receptor tyrosine kinase signaling in colorectal cancer cells via glycogen synthase kinase 3

Alina Starchenko[1], Ramona Graves-Deal[2], Douglas Brubaker[3], Cunxi Li[2], Yuping Yang[2], Bhuminder Singh[2], Robert J. Coffey[2], and Douglas A. Lauffenburger[1],*

[1]Massachusetts Institute of Technology, Department of Biological Engineering, Cambridge, MA, USA,
[2]Vanderbilt University Medical Center, Department of Cell & Developmental Biology, Nashville, TN, USA, and
[3]Purdue University, Department of Biomedical Engineering, West Lafayette, IN, USA

*Corresponding author: E-mail: lauffen@mit.edu

Abstract

As a key process within the tissue microenvironment, integrin signaling can influence cell functional responses to growth factor stimuli. We show here that clustering of integrin α5ß1 at the plasma membrane of colorectal cancer-derived epithelial cells modulates their ability to respond to stimulation by receptor tyrosine kinase (RTK)-activating growth factors EGF, NRG and HGF, through GSK3-mediated suppression of Akt pathway. We observed that integrin α5ß1 is lost from the membrane of poorly organized human colorectal tumors and that treatment with the integrin-clustering antibody P4G11 is sufficient to induce polarity in a mouse tumor xenograft model. While adding RTK growth factors (EGF, NRG and HGF) to polarized colorectal cancer cells induced invasion and loss of monolayer formation in 2D and 3D, this pathological behavior could be blocked by P4G11. Phosphorylation of ErbB family members as well as MET following EGF, NRG and HGF treatment was diminished in cells pretreated with P4G11. Focusing on EGFR, we found that blockade of integrin α5ß1 increased EGFR phosphorylation. Since activity of multiple downstream kinase pathways were altered by these various treatments, we employed computational machine learning techniques to ascertain the most important effects. Partial least-squares discriminant analysis identified GSK3 as a major regulator of EGFR pathway activities influenced by integrin α5ß1. Moreover, we used partial correlation analysis to examine signaling pathway crosstalk downstream of EGF stimulation and found that integrin α5ß1 acts as a negative regulator of the AKT signaling cascade downstream of EGFR, with GSK3 acting as a key mediator. We experimentally validated these computational inferences by confirming that blockade of GSK3 activity is sufficient to induce loss of polarity and increase of oncogenic signaling in the colonic epithelial cells.

Key words: systems biology; cell signaling; extracellular matrix; growth factor; receptors; integrin; tyrosine kinase; EGFR

INTEGRATION, INNOVATION AND INSIGHT

This study integrates quantitative experimental measurement of intestinal epithelial cell signaling pathway activities with phenotypic responses to a spectrum of growth factor and extracellular matrix stimuli, via computational modeling of the cue-signal-response relationships using a range of data-driven multivariate inference techniques. Insights gained from the study center on how multiple signaling pathways operate together to govern cell morphological responses to Integrin Alpha5 Beta 1 and EGF Receptor costimulation, with a key finding being a vital role for GSK3 in coreographing network pathway balances that influence intestinal epithelial cell function.

INTRODUCTION

Receptor tyrosine kinases (RTKs) are a large family of cell-surface growth factor receptors that govern many aspects of cell behavior [1, 2], a trait which makes them critical mediators of cancer development and progression. RTK signaling propagates via proximal nodes such Ras and PI3K [3–6] to downstream cascades of protein–protein interactions, culminating in a governance of a broad array of cellular responses. Sustained signaling through the ErbB (EGFR) and HGF families of receptors supports hyperproliferation and loss of apico-basolateral polarity, processes that support cancer progression [6–9]. For instance, EGFR can signal through the RAS/ERK and PI3K/Akt pathways [5, 10] with investigators commonly noting that a particular pathway may be predominant in a particular experimental set-up; however, the mechanistic reasons for these observations are not well understood.

Adhesion signaling through the integrin family of ECM receptors alters how a cancer cell integrates soluble growth factor cues into a phenotypic response [11–13]. Recent work suggests that, in addition to downstream nodes of crosstalk, direct interactions between integrin $\beta 1$ and EGFR have significant influence on EGFR signaling [14–17]. These effects can be both stimulatory as well as inhibitory to EGFR signal transduction, depending on the integrin $\beta 1$ heterodimerization partner as well as the EGFR-output measured. For instance, integrin $\alpha 5\beta 1$ seems to negatively regulate aspects of EGFR signaling in epithelial cells, whereas integrin $\alpha 2$ may be stimulatory [18–20]. Other studies show that integrin $\alpha 5\beta 1$ engagement leads to enhanced EGFR signaling [21, 22]. To complicate the picture further, still other studies suggest that integrin $\alpha 5\beta 1$ is able to alter the magnitude of the PI3K/Akt signaling cascade [23] downstream of EGFR in a manner that is controlled by expression of integrin $\alpha 5\beta 1$ in conjunction with cognate matrix ligands [24]. Such a body of competing hypotheses suggests context-dependent roles for integrin $\alpha 5\beta 1$ and highlights a need for an integrative computational analysis of how integrin $\alpha 5\beta 1$ signaling alters a cell's response downstream of EGFR activation.

In previous work, we showed that lateral clustering of integrin $\alpha 5\beta 1$ by the P4G11 antibody contributes to apico-basolateral polarity in invasive colorectal cancer (CRC) cells [25]. To advance these observations further, in our new work here we find that cell surface integrin $\alpha 5\beta 1$ correlates with apico-basolateral polarity in both human tumor and mouse xenograft model of CRC. Analyzing the integrated effects of activating RTK signaling and integrin $\alpha 5\beta 1$ in CRC cells, which normally exhibit a polarized phenotype when cultured in 3D type 1 collagen, we ascertain that concurrent treatment of EGF, HGF and NRG with the integrin $\alpha 5\beta 1$-clustering antibody mAb P4G11 abrogates the effect of these growth factors to induce loss of polarity and invasion. Based on measurements of key signaling pathway activities, we then constructed a machine learning-based model characterizing how P4G11 accomplishes this suppression, which yielded inference that clustered active integrin $\alpha 5\beta 1$ acts as a negative regulator of EGFR signaling via GSK3 as a key mediator.

MATERIALS AND METHODS

Antibodies

AIIB2 and P4G11 hybridomas were purchased from the Iowa Developmental Studies Hybridoma Bank. Antibodies were produced and purified by the Vanderbilt Antibody Core Facility (VAPR). P4G11 was used at 10 µg/ml in all studies, unless otherwise indicated. DyLight 594–conjugated P4G11 was produced by VAPR. Monovalent P4G11 F(ab)′ fragments were produced using the Ficin Digestion Kit from Millipore and conjugated to DyLight 594 by VAPR. Integrin $\alpha 5\beta 1$–blocking JBS5 was purchased from ThermoFisher (MA1-81134). Staining antibodies were Integrin a5, ThermoFisher (PA5-79529), E-cadherin, Abcam (ab40772), phalloidin-568 (A12380). All secondary antibodies were purchased from Invitrogen.

Cell lines

Details on derivation and culture of CC and SC cell lines from parental HCA-7 cell line are described in Li *et al.* [29]. These cells were cultured for a maximum of 10 passages. Caco-2 cells were purchased from ATCC and grown in DMEM supplemented with 10% FBS.

Animal studies

HCA-7 derived SC cells in PBS (10 million cells/mouse) were injected into nude mouse (Jackson labs) flank on right side and allowed to establish tumors and proliferate for 7 days until palpable. Mice were then treated with P4G11 (100µg/ml in saline, 200µg/mouse/dose total) or vehicle (saline. 200µl) via intraperitoneal injection every other day for three weeks. Tumors were then excised, cut in half, and fixed in either formalin and submitted for paraffin embedding or 4% paraformaldehyde.

3D type-1 collagen cultures

Briefly, 3D collagen sandwich assays were set-up using three layers of type-I collagen as previously described in detail [29]. Top and bottom layers consisted of 2 mg/ml collagen alone, and the middle layer consisted of 2 mg/ml collagen plus cells at 5000 cells/ml in a single-cell suspension. Collagen mixture was neutralized using sterile NaOH and each layer was neutralized

and allowed to polymerize before the next layer was added. All three layers contained 400 μl per well of a 12-well culture dish. Medium (400 μl) with or without reagents was added on top and changed every 2–3 days. Colonies were observed and counted after 14–17 days.

Collagen coating

Coverglass or Transwell filters were incubated with 0.3 mg/ml type-1 collagen in PBS for 30 min and rinsed twice with phosphate-buffered saline (PBS).

Tissue sections

Tumor xenografts or human tissues were fixed in 4% PFA, placed overnight in 30% sucrose, and frozen in OCT compound (TissueTech). Frozen blocks were cryosectioned into 6 μm sections, permeabilized with 1% Triton, and blocked with glycine (0.3 M, 30 min) and DAKO protein block (1 h) sequentially. Primary antibody was added overnight. Secondary antibodies from Invitrogen (Alexa Fluor-linked) were added at 1:1000 for 30 min. Slides were washed, mounted in Prolong (Life Technologies), and analyzed with confocal microscopy using a Nikon A1R LSM confocal microscope. H&E staining was performed by the VUMC histology core and imaged using a Leica SCS400 slide scanner.

3D immunofluorescence

Collagen sandwich was fixed in 4% paraformaldehyde (PFA) for 30 min at room temperature. Middle layer was removed and placed into IF buffer (1% BSA, 1% Triton X-100 in PBS) overnight. Alexa Fluor 568–phalloidin and 4′,6-diamidino-2-phenylindole (DAPI) were added for 4 h at 4°C before wash and confocal microscopy on Nikon A1R. For immunofluorescence, primary antibodies were added at 1:200 overnight in IF buffer. Samples were then washed, and secondary antibody was added at 1:1000 for 1 h at 4°C. Samples were washed and whole mounted onto a #1.5 glass coverslip and subsequently analyzed using confocal microscopy on a Nikon A1R LSM.

Colony counting

Colonies were counted using GelCount (Oxford Optronix) with identical acquisition and analysis settings and represented as mean from triplicates ± SEM. For cystic and invasive morphology, counts were performed manually from three individual wells and represented as mean ± SEM.

Luminex assay and sample preparation

Cells were plated in 96-well plates coated with monomeric type-1 collagen and grown for 5 days under indicated conditions. For short-term signaling experiments, cells were treated with indicated antibody or inhibitor treatment in 2% serum-containing media for 4 h prior to addition of growth factor. Following growth factor addition, cells were kept at 37°C for indicated length of time and then reaction was stopped with a fast rinse of 4°C PBS followed by addition of 4°C Luminex cell lysis buffer. Cells were lysed for 30 min at 4°C on an orbital shaker and centrifuged at 14000 g for 10 min. Ten microliter of lysate was used for each Luminex reaction with a total volume of 50 μl in a 384-well plate. Beads were incubated with lysate and assay buffer overnight at 4°C followed by washing and addition of secondary antibody for 30 min and PE for 15 min. Samples were washed and read on a Bio-plex 3D suspension array system Luminex reader. Long-term experiments utilizing GSK3a/b inhibitor CHIR99021 used a 10 nM concentration for five days. Short-term Luminex experiments utilized a concentration of 10 nM pretreatment for 1 h prior to EGF addition and signaling analysis.

Partial least-squares analysis

Partial least-squares discriminant analysis (PLSDA) and partial least-squares regression (PLSR) were performed using the MATLAB PLS Toolbox (Eigenvector Research, Inc.). Data were normalized along each X and Y parameter by Z-score before application of the algorithm. Cross-validation was performed with one-third of the relevant dataset. The number of latent variables (LVs) was chosen so as to minimize cumulative error over all predictions. We orthogonally rotated the models so that maximal separation was achieved across LV1 where noted. We calculated model confidence by randomly permuting Y 100 times and rebuilding the model to form a distribution of error for these randomly generated models. We compared our model to this distribution with the Mann–Whitney U-test to determine the significance of our model. The relative contribution of each parameter to the overall model prediction was quantified using Variable Importance in Projection (VIP) score. A VIP score > 1 (above average contribution) was considered important for model performance and prediction.

Partial correlation analysis

Cytokine data from Luminex measurements were transformed using a z-score. Networks were constructed in R (64bit, version 3.43) with the GeneNet package [26, 27]. We constructed networks for Luminex measurements from CC cells pretreated with 10μg/ml P4G11 or JBS5 and/or and 10 nM GSK3a/b inhibitor CHIR99021 in the presence or absence of 10 ng/ml EGF (Visualization thresholds: p < 0.05 and/or FDR-based probability >0.80).

RESULTS

Surface clustering of Integrin α5ß1 correlates with less malignant tumors in vivo

Although downstream crosstalk between RTK and integrin signaling pathways is well documented [28], the role of integrin clustering in this crosstalk has not been well described. Our previous work shows that clustering of integrin α5ß1 on the surface of invading CRC cells reduces their migration and restores epithelial polarity in vitro [25]. To ascertain if surface integrin α5ß1 is lost from the surface of human CRC cells in vivo, we obtained tumor and adjacent normal tissues from three patients and used immunofluorescence to determine the localization of integrin α5ß1 and E-cadherin. Figure 1A shows their distribution in a representative region of tumor and adjacent normal tissue. We note that although integrin α5ß1 is present at the lateral surface of differentiated colonic epithelial cells as previously described, this lateral staining is absent from the tumor. These data suggested that surface integrin α5ß1 is not only important in guiding epithelial morphogenesis in vitro but may also contribute to aspects of CRC progression.

To further explore the effects of integrin α5ß1 clustering on colorectal cell invasion in vivo, we treated invasive SC mouse tumor xenografts with integrin α5-activating and clustering antibody P4G11. SC cells were injected subcutaneously into the
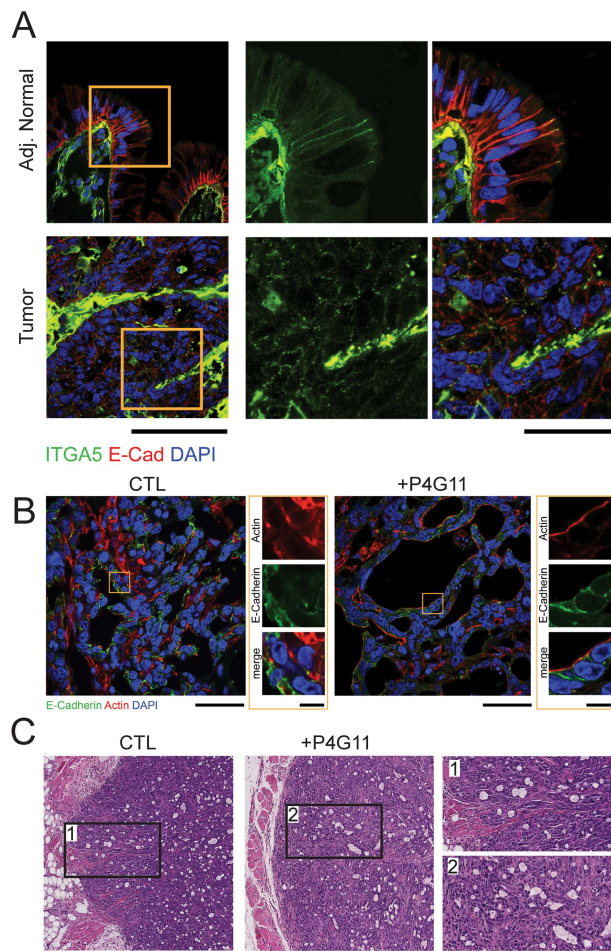
Figure 1. Presence of Integrin α5ß1 at lateral cell–cell junctions correlates with increased epithelial organization *in vivo*. (A) FFPE sections from human colorectal cancer tumors and adjacent normal regions were stained for integrin α5 (green), E-Cadherin (red), and DAPI (blue) (B–C) HCA-7-derived SC cells were injected subcutaneously into nude mice and allowed to establish palpable tumors (1 week). Mice were subsequently given P4G11 or vehicle via intraperitoneal injection for 21 days (B) Representative confocal images of SC tumor sections stained with antibody against E-Cadherin (green), Phalloidin (red) and DAPI (blue). Scale bar = 50um. Inset scale bar = 10um. Note appearance of basolateral anti-mouse secondary antibody binding in P4G11-treated tumors. (C) Representative histology of control and P4G11-treated tumors, scale bar = 500um, inset scale bar = 50uM.

flank of a nude mouse and allowed to establish tumors over three weeks. Mice were then treated with 100 µg/ml of P4G11 three times a week for three weeks at which point tumors were excised and analyzed. To determine if P4G11 treatment induces a higher level of apico-basolateral polarity, we examined the distribution of E-cadherin and actin in FFPE sections. We find that most lumens in P4G11-treated tumors are surrounded by cells that exhibit epithelial polarity (Fig. 1B) whereas lumens in untreated tumors are surrounded by disorganized cells that do not. We also observed diminished invasion in P4G11-treated animals, although the small number of mice in the experiment made it difficult to draw statistically meaningful conclusions (Fig. 1C). These data led us to conclude that clustering integrin α5ß1 at the cell surface negatively regulates aspects of tumor growth and organization *in vivo* and supported the possibility of signaling changes downstream of P4G11-mediated integrin clustering.

Surface clustering of Integrin α5ß1 via P4G11 blocks growth factor-induced loss of polarity and invasion in vitro

We next endeavored to understand how integrin clustering produces the phenotypic behaviors described above. Since RTK signaling is a strong driver of invasion and drug resistance in human adenocarcinoma cell lines such as HCA7 and its derivatives CC and SC [29], we hypothesized that P4G11's ability to enhance epithelial cell polarity and attenuate cell invasion *in vivo* and *in vitro* could be due to negative regulation of RTK signaling through integrin α5ß1 clustering.

To test whether P4G11 dampens RTK signaling, we treated CC cells in type-1 collagen over the course of 15 days with EGF, NRG and HGF with 10 µg/ml P4G11 as previously described [29]. Cell colonies were then fixed and stained with phalloidin and DAPI, then their morphology was analyzed using fluorescent confocal microscopy. Individually each of these three growth factors is sufficient to induce a loss of polarity and produce an invasive phenotype in CC cells in 3D (Fig. 2A). Interestingly, treatment of CC cells with growth factors and P4G11 together is sufficient to block invasion, loss of cystic architecture, and loss of epithelial polarity (Fig. 2A–C). To ascertain that P4G11 is not simply blocking integrin α5ß1 activity, we compared the P4G11 phenotype to that of integrin ß1 blocking antibody AIIB2 and found that, although blocking integrin ß1 additionally blocks invasion, it also leads to a loss of lumen formation (Fig. 2D). We have previously shown that P4G11 antibody bivalency is necessary for clustering and activation of integrin α5ß1 and only bivalent P4G11 is able to induce epithelial polarity and block invasion in CRC cells [25]. To confirm the mechanism underlying P4G11-mediated RTK-ligand blockade occurs only with bivalent antibody, we used a monovalent P4G11 F(ab) fragment that binds integrin but cannot cluster it. P4G11 F(ab) is unable to block growth factor-induced loss of epithelial polarity or invasion (Fig. 2E, F). These data led us to conclude that integrin α5ß1 clustering by P4G11 blocks RTK-induced invasion and loss of epithelial polarity in type-1 collagen to create a 3D environment.

Surface clustering of Integrin α5ß1 negatively regulates RTK receptor phosphorylation

We next sought to determine the molecular mechanism underlying the ability of P4G11 to block CRC cell disorganization and invasion following RTK stimulation. There are many cellular mediators of integrin-RTK crosstalk that work together to integrate mechanical and chemical stimuli into a single behavioral phenotype (Fig. 3A). To measure the effect of P4G11 on cellular kinases involved in RTK signal transduction, we first altered our assay platform to a 2D Monomeric collagen (MMC)-coated substrate. Focusing initially on EGF-elicited effects, we confirmed that P4G11 is able to rescue EGF-mediated loss of polarity in 2D (Fig. 3B). We then used a Luminex-based assay to measure the phosphorylation of several RTK family members in response to a 5-minute stimulation with 20 ng/ml EGF, NRG or HGF following a 4-hour pretreatment with 10 ug/ml P4G11. We find that pretreatment with P4G11 results in significant reduction in levels of phosphorylated ErbB family members EGFR, ERBB2 and ERBB3 as well as phosphorylated MET receptor (Fig. 3C and D). Taken together, these observations indicate that integrin α5ß1 clustering is a broad negative regulator of RTK phosphorylation, particularly that of ErbB family members.
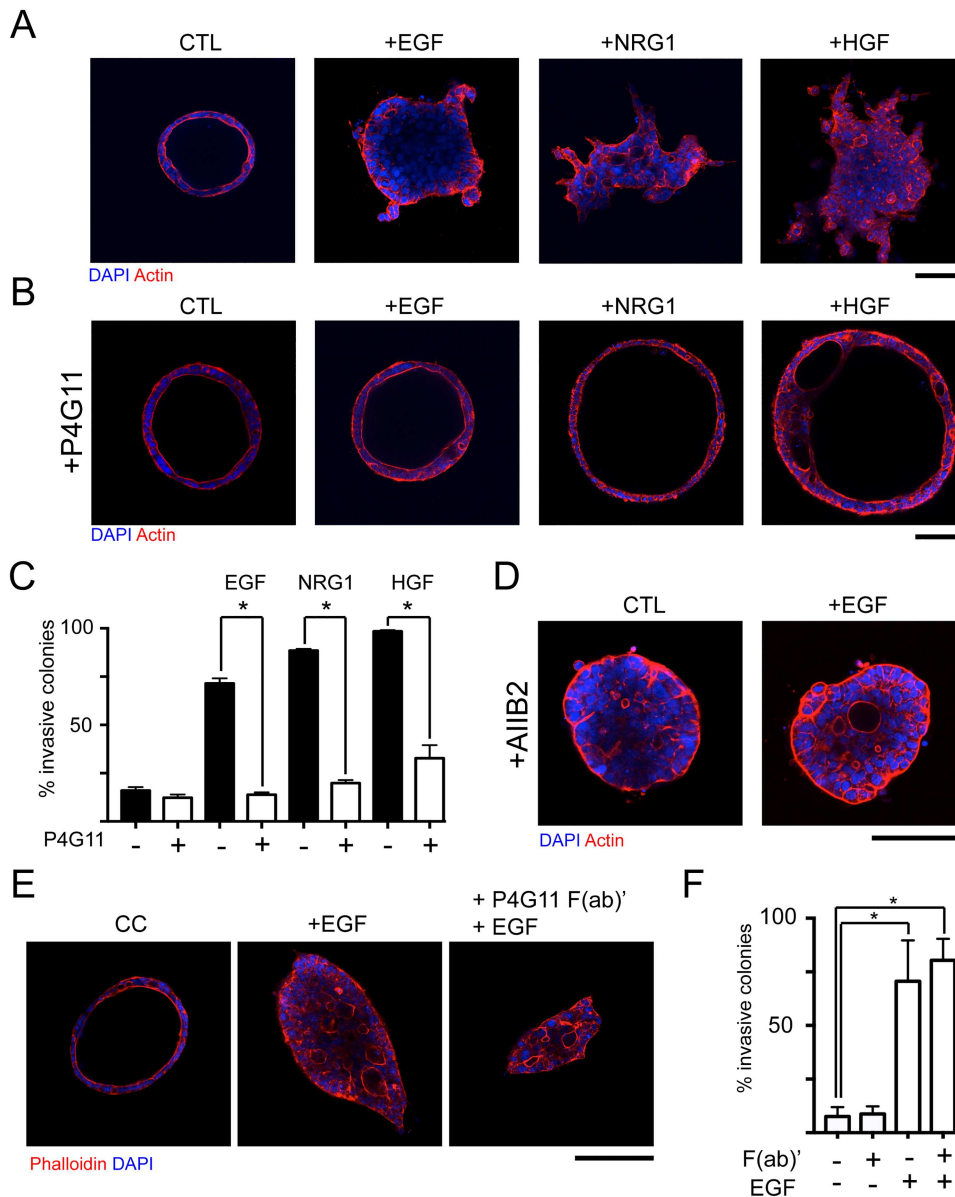
Figure 2. Surface clustering of Integrin α5ß1 via P4G11 blocks growth factor-induced loss of polarity and invasion *in vitro* CC cells were cultured for 15 days in 3D type 1 collagen and treated as indicated on days 8–15, fixed, stained with DAPI (blue) and Phalloidin (red), and imaged on a Nikon A1R confocal. **(A)** Representative confocal images of CC colonies after treatment with 20 ng/ml EGF, NRG1, or HGF on days 8–15 or **(B)** cotreatment with the indicated ligand and 10µg/ml mAb P4G11 on days 8–15. **(C)** Quantification of the percentage of CC exhibiting an invasive colony phenotype post-treatment with EGF, NRG1 or HGF (black) or after cotreatment with ligand and P4G11 (white) (mean ± SEM; *n* > 400 colonies from four separate replicates). **(D)** Representative confocal images of CC treated with ITGß1 blocking mAb AIIB2 on days 8–15 alone or in concert with EGF stained with DAPI (blue) and Phalloidin (red). **(E)** Representative confocal images of CC colonies following treatment with EGF or EGF plus P4G11 F(ab)′ fragment **(F)** Quantification of the percentage of CC exhibiting an invasive colony phenotype post-treatment with EGF or EGF and P4G11 F(ab)′ fragment. Scale bars = 50um unless otherwise indicated. P-value calculated by standard two-sided T-test and is <0.01 where indicated by asterisk (*).

Integrin activation and clustering are complex biochemical events involving both changes in conformation and action of focal adhesion proteins [30]. Hence, we wanted to determine if other means of altering integrin α5ß1 activity would also alter RTK signaling. We continued to put primary focus on the EGF–EGFR pathway because it yields the most robust phenotypic effects, involves the best characterized receptor components, and can be analyzed with the most specific reagents. To test whether blocking integrin α5ß1 activity is sufficient to increase EGFR signaling, we repeated the phosphoproteomic analysis using the integrin α5ß1 blocking antibody JBS5, which stabilizes

the inactive conformation of integrin α5ß1 [31, 32]. We found that 4-hour treatment with JBS5 is sufficient to significantly increase baseline phospho-EGFR levels, but it does not significantly alter response to acute EGF treatment (Fig. 3E). Since the increase in phospho-EGFR following short-term integrin α5ß1 inhibition is minor but present, we tested the effect of long-term integrin α5ß1 inhibition on phospho-EGFR and ErbB2 in the presence or absence of 20 ng/ml EGF. We find that continuous inhibition of integrin α5ß1 over 3 days is sufficient to significantly raise baseline p-EGFR, p-ErbB2 and p-Met (Fig. 3F, Supplementary Fig. 1). This effect is amplified in cells cotreated with JBS5 and EGF
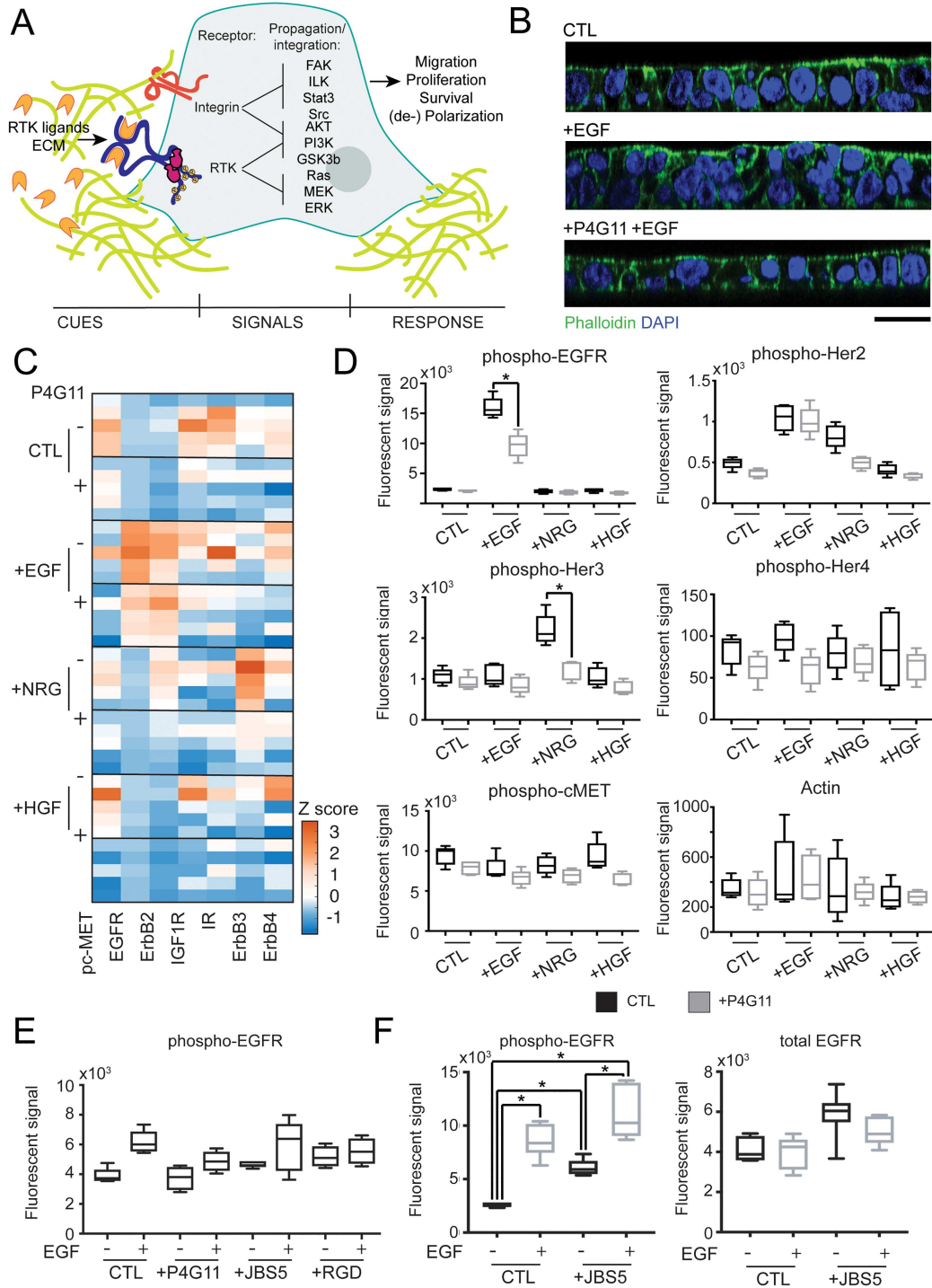
Figure 3. Surface clustering of Integrin α5ß1 negatively regulates RTK receptor phosphorylation in CC cells in 2D. Signaling at the receptor level was analyzed in CC cells grown on 2D MMC-coated substrates in the presence of different Integrin α5ß1 and RTK treatments. **(A)** Rudimentary schematic of players involved in the signaling between tyrosine kinase and integrin receptor families. **(B)** CC cells were grown on Transwell filters for 5 days in the presence of EGF or EGF with P4G11, fixed, stained with phalloidin (green) and DAPI (blue), and imaged using an A1R confocal microscope. **(C)** Heatmap summary of z-score normalized Luminex measurements of phosphorylated RTK family members in CC cells pretreated with P4G11 and then stimulated for 5 min with EGF, NRG or HGF. Each block represents the value of a single phospho-kinase in a single biological replicate; thus each row is a single biological replicate. Z-score was calculated per analyte. **(D)** Graphical representation of measurements from (C). **(E)** CC cells were treated with P4G11, JBS5 or RGD for 4 h and stimulated with EGF for 5 min. Phospho-EGFR was measured using Luminex assay. **(F)** CC cells were grown in the presence of JBS5 and EGF for 5 days and then the amount of phospho-EGFR was measured by Luminex. P-values calculated by standard two-sided T-test and is $P < 0.05$ where indicated by asterisk (*).

for the same 3-day period. These data support the model that integrin α5ß1 activity negatively regulates response to EGFR signaling and that loss of integrin α5ß1 regulation pushes the CC cells to a higher state of EGFR signaling.

PLS-DA modeling implicates GSK3 in the dampening process

We have shown that treatment of CC cells with P4G11 reduces their responsiveness to RTK-ligand activation, pointing to a broad RTK-dampening activity of clustered integrin α5ß1. We next wanted to determine what components of EGFR signaling play a role in this process. To determine what EGFR-pathway kinases are downstream of integrin α5ß1 regulation, we repeated the acute stimulation experiments from Fig. 3 and measured phosphorylation of key protein nodes within multiple kinase pathways downstream of RTK activation in the presence and absence of P4G11 via the Luminex-based assay. We observed a highly heterogenous response, and although a general pattern of P4G11-mediated reduction in pS/T Akt, pS/T MEK and pS/T GSK3 was observed it gave inadequate statistical significance (Fig. 4A and B).

Biological signaling networks involve multiple pathways comprising nodes exhibiting highly correlated activities along with diverse patterns in response to stimulation. In order to identify key kinases responsible for mediating the P4G11-elicited response, we employed a machine learning approach known as Partial Least-Squares Discriminant Analysis (PLS-DA) [33]. PLS-DA is used to identify combinations of variables (e.g. phosphorylated kinases) that are statistically significant in predicting a categorical group (e.g. P4G11 treated or untreated) when no single variable is sufficient as a result of the inherent co- and anticorrelations among nodes within RTK-mediated signaling networks. The outcome of a PLS-DA model is termed a LV, which is a weighted combination of measured variables (phosphorylated kinases). In this set of experiments, the directionality and magnitude associated with each variable (phosphorylated kinase) corresponds to the importance of this variable (kinase) in predicting if the sample was treated with P4G11 or not, which is quantified as the VIP score.

We began by building a single aggregate PLS-DA model of kinase activation to predict whether or not cells were treated with P4G11, based on the node activity patterns. This approach did not result in a statistically significant model due to the disparate nature of patterns generated by EGF, NRG and HGF (Supplementary Fig. 2). Thus, in an aggregate model there was too much variation contributed by the growth factors compared to that contributed by P4G11 and this model would be difficult to interpret to better understand P4G11 effects. Therefore, we instead constructed individual PLS-DA models, respectively corresponding to each treatment, toward determining which kinases were most predictive of samples treated with P4G11 over each of the four conditions separately. Figure 4C shows that we are indeed able to build four statistically significant models to predict which samples were treated with P4G11 based on the phosphorylation of downstream kinases. The values of each kinase on LV1 are shown in Fig. 4D. The only kinase with a significant VIP score across all four models is GSK3 (Fig. 4E). GSK3 phosphorylation is anticorrelated with the presence of P4G11. This result suggests GSK3 may be involved in P4G11-mediated dampening of RTK signaling. Although GSK3β is the most highly expressed GSK3 family member in epithelial cells and therefore a likely mediator of this process, the reagents used

in this study do not adequately differentiate between GSK3α or GSK3β, and as such we will refer to the molecule simply as GSK3.

GSK3 inhibition is sufficient to induce loss of epithelial organization and apical-basolateral polarity

GSK3 is a tumor suppressor protein in epithelial cells, as a multifaceted kinase with hundreds of predicted substrates [34]; one facet of its influence is in conjunction with Wnt signaling. GSK3-mediated β-catenin phosphorylation leads to degradation of the latter with consequent inhibition of Wnt signaling effects [35].Phosphorylation of GSK3 leads to its inactivation. GSK3 has also been identified as a broad negative mediator of signaling downstream of RTK family members, possibly through its ability to enhance PTEN activity and reduce Akt signaling [36]. Additionally, GSK3 is able to phosphorylate focal adhesion kinase (FAK) in a manner that favors dynamic turnover of cell/substratum adhesions during cell migration [37]. Taken together this all raises the notion that GSK3 is a key mechanistic mediator via which EGFR signaling effects are diminished by P4G11.

Our signaling data shown in Fig. 4 led us to hypothesize that the effects of GSK3 are deactivated by growth factor signaling, and this deactivation is blocked by P4G11. GSK3 has previously been reported to regulate epithelial junction formation and maintenance [38]. To test whether inhibiting GSK3 activity is sufficient to induce a loss of epithelial polarity, we cultured CC and Caco-2 cells in the presence of CHIR99021, a potent inhibitor of both GSK3a and GSK3b activity [39], for three days on Transwell filters coated with MMC. Inhibition of GSK3 resulted in disruption of monolayer formation, creating a multilayered phenotype in both cell lines (Fig. 5A).

We next sought to understand how GSK3 inhibition alters signaling downstream of EGF stimulation in CC cells. To do this, we measured the phosphorylation of 19 major kinase nodes in pathways downstream of EGFR using Luminex following a 5-minute EGF stimulation after a 4-hour treatment with CHIR99201 (GSKi) with or without P4G11. Surprisingly, we found few obvious differences in signaling following GSK3 inhibition across all samples. Notably, phosphorylation of p38 was slightly elevated with GSK3 inhibition, whereas phosphorylation of p70s6 was decreased, as was that of its substrate S6RP (Supplementary Fig. 3). To enhance insights from this complex compendium of measurements we built a PLS-DA model to elucidate the identities of kinase activities that most substantively covary with GSK3 inhibition in presence and absence of P4G11 following EGF treatment (Fig. 5B). We found that performing PLS-DA with four categorical groups (EGF, EGF + P4G11, EGF + GSKi, and EGF + P4G11 + GSKi) separates the data most strongly on whether the samples were treated with GSKi (LV1). Examining the loadings on LV1, we found that BAD, JNK, p38 MAPK, Src, and STAT3 were most strongly associated with GSK3 inhibition. Moreover, the LV1 scores in this model are consistent with how strongly polarizing cells are shifted to an unpolarized phenotype, with P4G11 + EGF treated cells having more negative scores on LV1 and EGF + GSKi having more positive scores compared to all samples.

Despite the complexity of response to GSK3 inhibition, we sought to test whether signaling outcomes of GSK3 inhibition covary with cancer-promoting signaling. We performed a PLSR analysis to determine if higher levels of inactive phospho-GSK3 levels covaried with higher RTK pathway signaling, similarly to our previous demonstration of this approach for epithelial cell adhesion and migration [40]. Here, the PLS approach was used
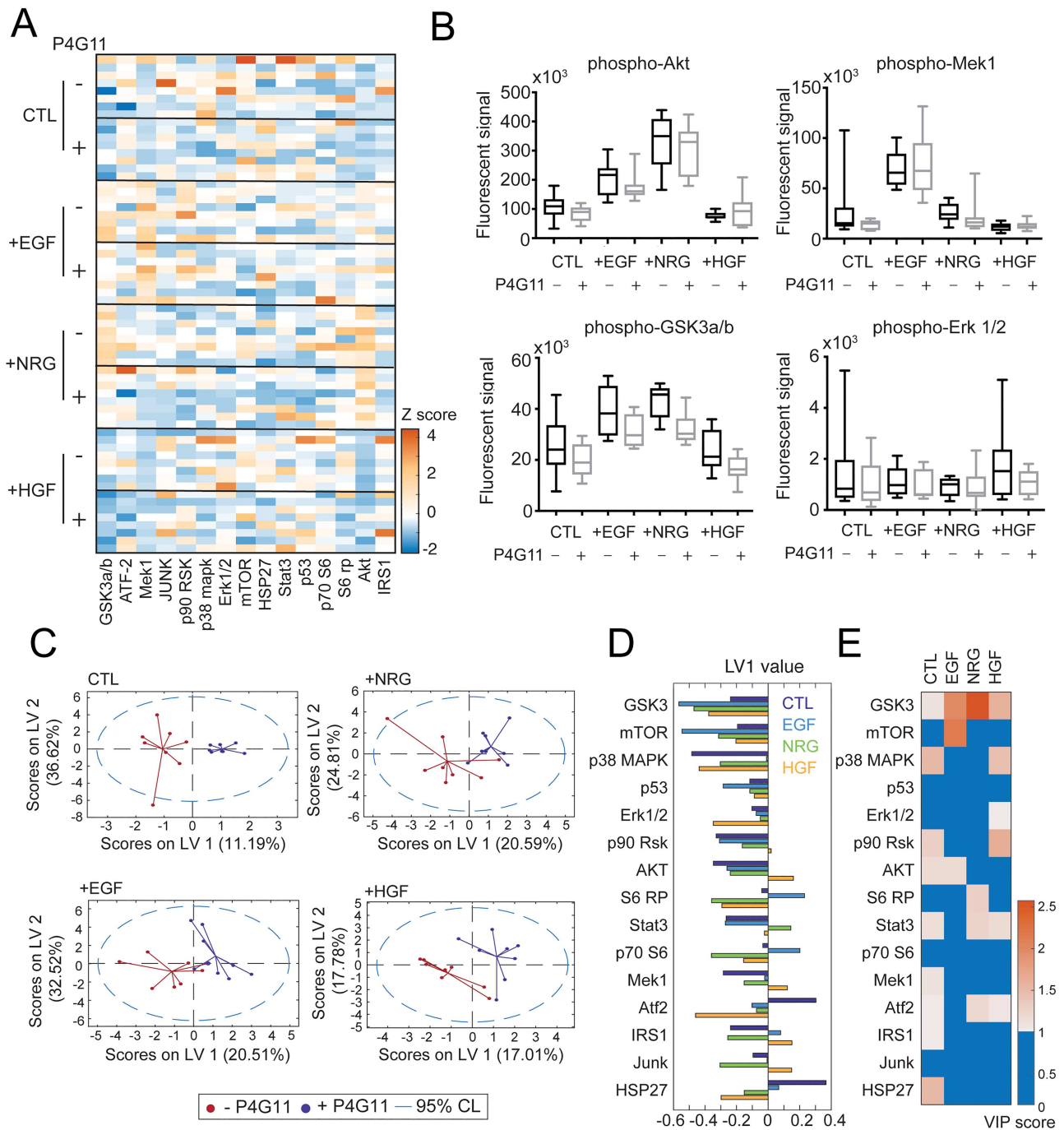
Figure 4. PLS-DA modeling of signaling downstream of EGF reveals P4G11-specific signatures and implicates GSK3 as a downstream player. CC cells were grown on 2D MMC-coated substrate, incubated with P4G11 for 4 h, and then treated with EGF for 5 min. Phosphorylation state of kinases downstream of EGFR family members and Met was measured by Luminex. **(A)** Heatmap summary of z-score normalized Luminex measurements of phosphorylated RTK-signaling pathway members in CC cells pretreated with P4G11 and then stimulated for 5 min with EGF, NRG or HGF. **(B)** Graphical representation of selected measurements from (A). Notably, no single difference between P4G11 treated and untreated samples were statistically significant across any one kinase we measured when using a standard T-test analysis and a $P < 0.05$ cutoff. **(C)** Four separate PLS-DA models were trained corresponding to each growth factor. Shown are scores plots for the samples in LV1 and LV2 space; variance explained refers to the predictor variables. Each dot represents the score of the function applied to a single biological replicate. **(D)** Summary of loadings from each model. Negative values covary with growth factor alone, and positive loadings covary with P4G11 treatment. **(E)** Variable Importance in Projection (VIP) scores were calculated for each kinase in each model, and these are summarized here. Shown are VIP scores above 1, as that is the significance cutoff.

to determine which combination of phosphorylated kinases was quantitatively (rather than categorically, as is the utility of PLS-DA) predictive of a high level of GSK3 inhibition following EGF treatment. We used the level of phospho-GSK3 as the response variable and the other kinases as measured variables. We find that high activity through both Akt and ERK pathways is predictive of a given sample having high inactive GSK3 (Fig. 5B), implicating a key contribution by GSK3 in regulation of RTK
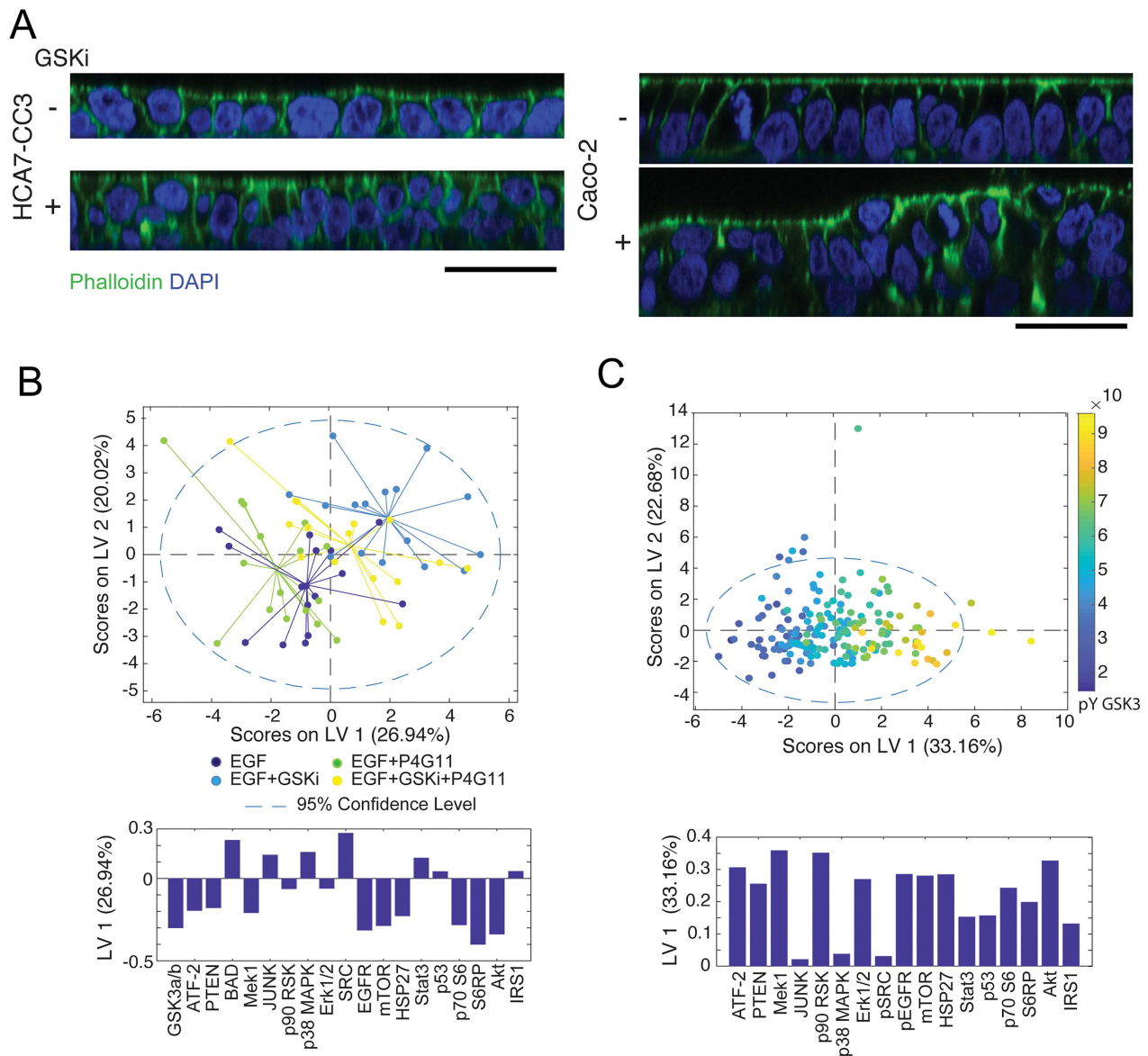
Figure 5. GSK3α/β inhibitor is sufficient to induce loss of polarity with or without P4G11. (A) CC cells were grown on 2D MMC-coated substrates and treated with GSK3 inhibitor 10 nM CHIR99021 for 5 days. Cells were fixed and stained with Phalloidin (green) and DAPI (blue) and examined using a Nikon A1R microscope to ascertain their ability to form a monolayer. **(B)** PLS-DA was used to build a model to predict perturbation ID based on phosphorylated kinase activity. Shown are the scores plot of the samples in the plane of LV1 and LV2, color-coded by the treatment combination and the loadings plot showing the direction and magnitude of the covariance for each kinase included in the model. **(C)** PLS-R analysis was used to determine which combination of phosphorylated kinases covaried with high levels of inactivation p-GSK3. Shown are the scores plot of the samples in the plane of LV1 and LV2, color-coded by the measured level of phosphorylated GSK3 and the loadings plot showing the direction and magnitude of the covariance for each kinase included in the model; variance explained refers to the predictor variables.

signaling pathways, with its inhibition is sufficient to induce loss of polarity in CRC cells.

Integrin α5ß1 modulates signaling crosstalk downstream of EGFR through GSK3 and PTEN

The results described above render evident that phenotypic changes in cell behavior can arise from heterogenous modest changes in activities within multiple kinase pathways instead of critically by large changes in any individual pathway. Partial correlation analysis offers a mathematical tool for assessing how quantitative associations between pairs of proteins

are affected by diverse perturbations that broadly have largely activating or inhibiting effects across a highly correlated network [41]; this enables inference of the most strongly coupled nodes.

We hypothesized that clustered integrin α5ß1 serves as a negative regulator of EGFR signaling in polarized epithelial cells and that this regulation occurs in part through integrin α5ß1 blocking deactivation of GSK3 following EGF stimulation (Fig. 6A). To determine whether modulating integrin α5ß1 activity alters direct relationships between kinases downstream of EGFR, we pretreated CC cells with integrin α5ß1 clustering antibody P4G11 or integrin α5ß1 blocking antibody JBS5 for
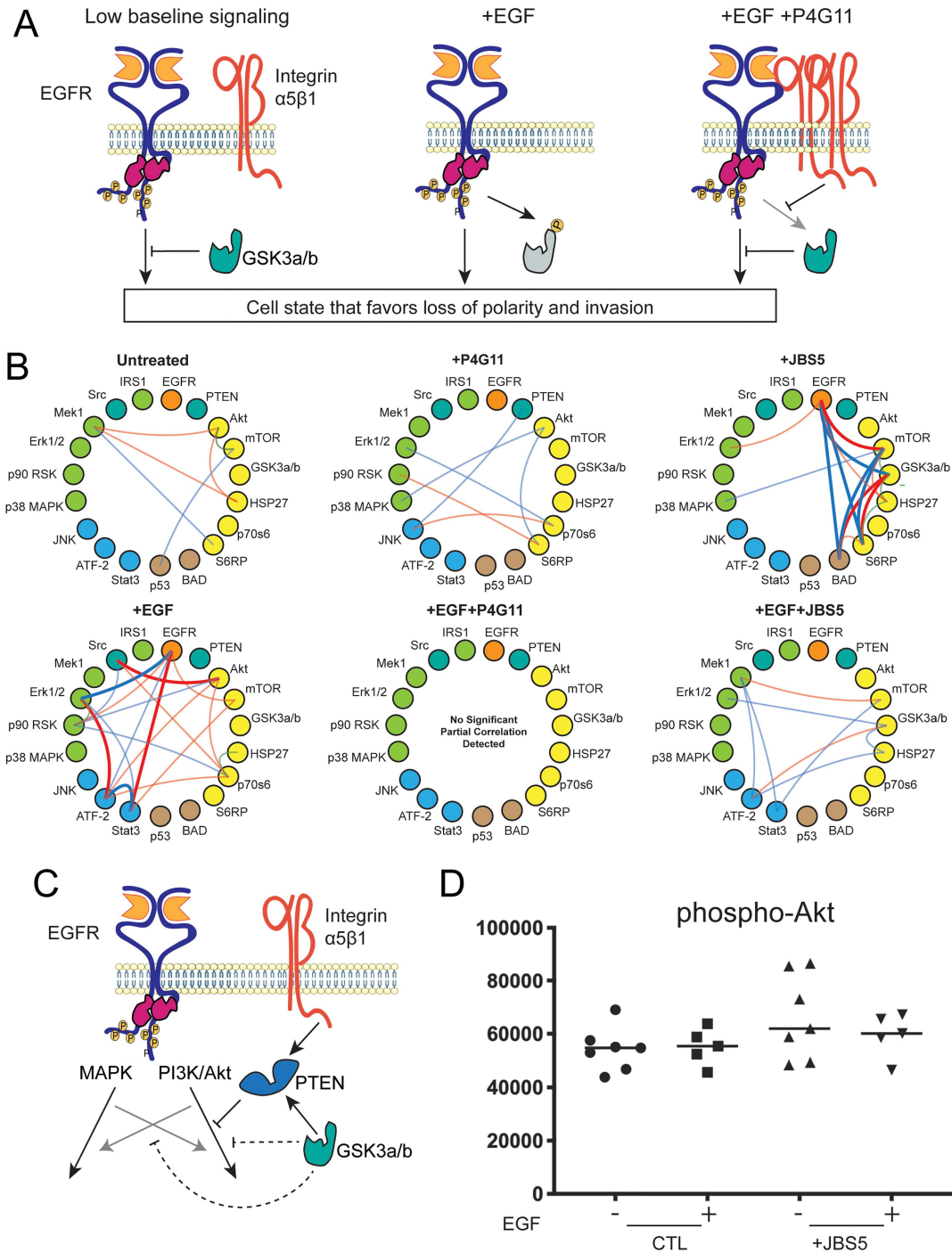
Figure 6. Partial correlation analysis shows Integrin α5ß1 is a negative regulator of EGFR signaling through Akt. (A) Hypothetical negative modulation of EGFR signaling by Integrin α5ß1 via GSK3 (B) CC cells were cultured on 2D MMC-coated substrates and treated with P4G11 or JBS5 for 4 h prior to a 5-minute treatment with 20 ng/ml EGF. Kinase phosphorylation was measured by Luminex. Partial correlation analysis for selected treatments was performed, and the statistically significant edges are visualized here. Thick edges have a significant P ($P < 0.05$) and an FDR-based probability measure of greater than 0.80; thin edges only have a $P < 0.05$ and are less significant. Kinases are loosely organized and color-coded by pathway. Red edges indicate negative correlations and blue edges indicate positive edges. Full set of results for all treatment combinations can be found in supplement. (C) Refined model of how Integrin α5ß1 negatively modulates Akt signaling and pathway crosstalk downstream of EGFR. (D) CC cells were grown on 2D MMC-coated substrates in the presence of JBS5 with or without EGF for 5 days. Akt phosphorylation was measured by Luminex.

4 h and then performed a 5-minute stimulation with EGF. We measured phosphorylation of 19 kinases in the EGFR pathway by Luminex (Supplementary Fig. 3) and used partial correlation analysis to uncover the most significant node–node activity couplings (Fig. 6B). Little baseline association is uncovered in untreated and P4G11-treated cells, but blocking integrin
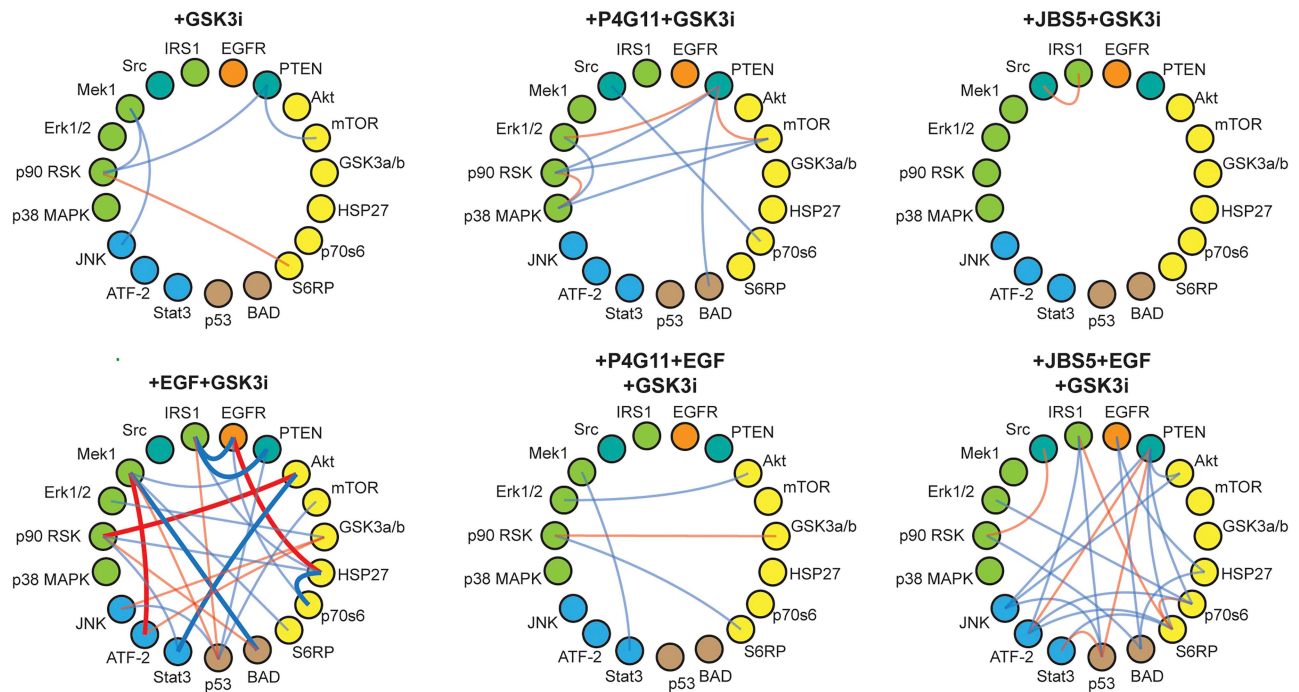
Figure 7. Partial correlation analysis shows GSK3α/β inhibition potentiates EGFR signaling downstream of Integrin α5ß1. (A) CC cells were cultured on 2D MMC-coated substrates and treated with P4G11, JBS5, or CHIR90021 for 4 h prior to a 5-minute exposure to 20 ng/ml EGF. Kinase phosphorylation was measured by Luminex. Partial correlation analysis for selected treatments was performed and the statistically significant edges are visualized here. Thick edges have a significant P (P < 0.05) and an FDR-based probability measure of greater than 0.80; thin edges only have a P < 0.05 and are less significant. Kinases are loosely organized and color-coded by pathway. Red edges indicate negative correlations and blue edges indicate positive edges.

α5ß1 with JBS5 yield results in significant activity associations between EGFR and members of the Akt pathway in the absence of EGF. In the presence of EGF alone, we find a positive association between EGFR and Erk1/2 and a negative association between EGFR and Stat3; these associations disappear in P4G11-treated cells. Intriguingly, coupling appears between members of the Akt and Mek signaling pathways in CC cells treated with both EGF and JBS5 (Fig. 6C and D; Supplementary Fig. 3).

To test whether GSK3 plays a role in negatively regulating RTK signaling downstream of integrin α5ß1 clustering, we repeated the above studies in the presence of CHIR99021. Again, signaling network node phosphorylation changes were found (Supplementary Fig. 3), and partial correlation analysis was performed (Fig. 7). Treatment of cells with both EGF and CHIR99021 yields a highly interconnected network compared to EGF treatment alone, suggesting that GSK3 does negatively regulate crosstalk between Akt and MEK/ERK signaling cascades downstream of EGFR activation. When GSK3 activity is inhibited, P4G11 is not able to reduce the associations between Akt and MEK/ERK pathway members as strongly as P4G11 alone following EGF treatment, but CHIR99021 is not able to fully block P4G11-mediated loss of all network associations. The inability of GSK3 inhibition to block all P4G11 dampening effects suggests that P4G11-mediated integrin α5ß1 clustering results in signaling or signal modification that is not completely GSK3-dependent.

Summarizing these modeling-derived insights, GSK3 inhibition in the presence of integrin α5ß1 inhibition leads to a loss of the Akt pathway heavy connections present in just JBS5-treated cells. A major role for GSK3 in choreographing signaling downstream of integrin α5ß1 is highlighted. Inhibiting activities of both GSK3 and integrin α5ß1 in the presence of EGF yields greater

overall correlation across the multiple pathways, indicating that the effect of GSK3 is to shift quantitative weights of various pathways in diverse treatment contexts.

DISCUSSION

In this study, we have addressed how integrin α5ß1 clustering generates downstream signaling crosstalk that suppresses RTK signaling-induced colonic epithelial cell behavior, such as loss of polarity and increased migratory invasion. Our approach uses integrin α5ß1 clustering antibody P4G11 as a tool to modulate the relevant signaling activities, multiplex measurement of key signaling phosphoprotein nodes, and multivariate computational techniques, to elucidate signaling network relationships associated with the downstream consequences of clustering. Our central finding is that RTK-elicited activation of the Akt pathway is diminished by α5ß1 clustering and that this amelioration is critically governed via GSK3.

Because of this network pathway crosstalk complexity, we employed partial correlation analysis to help elucidate our key insights as illustrated in Figs. 6 and 7. Partial correlations characterize the quantitative relationships between any two nodes in the integrin α5ß1 / RTK signaling network after accounting for their shared correlations with all the other nodes. For instance, looking at Fig. 6B for EGF treatment conditions, there are multiple strong partial correlations—some positive, some negative—between certain nodes. These represent significant heterogeneity among pathway node interactions induced by EGF treatment, which this modeling technique reveals underneath a more general overall activation of the network broadly. As examples, the interaction between EGFR and ERK elicited by EGF treatment is substantially further strengthened relative to the

overall network activation, whereas the interaction between Src and Akt becomes relatively weakened. Similarly, one can see in Fig. 7 the interactions between GSK3 and various other signaling nodes becomes relatively weakened upon treatment with the GSK3 inhibitor.

Addition of P4G11 is then seen to abrogate this heterogeneity, implying that even though the network is activated broadly by EGF, the clustering of α5ß1 integrin renders the balance among the various pathways to be more homogeneous. It can be inferred, accordingly, that an imbalance among certain pathways downstream of EGF is required for loss of epithelial polarity and enhanced invasive migration. Integrin α5ß1 blocking antibody JBS5 also invokes alternative diversifications of pathway activities especially with respect to GSK3; these heterogeneities are largely mitigated by EGF treatment, especially that of an otherwise negative partial correlation between EGFR and GSK3 activities. This finding suggests that GSK3 may be a particularly critical node for modulating phenotypically germane pathway activity imbalances—which is observed experimentally (Fig. 5). Comparing Fig. 7 to Fig. 6B, a GSK3 inhibitor dramatically modulates the strongest node–node associations under all treatment conditions.

The notion that integrin α5ß1 can regulate Akt downstream of EGFR has been previously reported, but only in the context of knockout or overexpression studies; overexpression of integrin α5 can lead to increased levels of Akt signaling whereas knockout of α5 or β1 leads to a reduction of Akt signaling [42–44]. Although this seems counter to our observation, it is in line with previous work showing that integrin α5ß1 in a stabilized adhesion functions to promote epithelial polarity [25, 45, 46]. Recent studies further implicate integrin recycling as intricately involved with epithelial polarity and differentiation by targeting a protein involved in integrin trafficking post internalization [47], and that EGFR signaling requires coordinate recycling with integrin ß1 via Rab-coupling protein RCP [15]. We speculate that because integrin α5ß1 can mediate EGFR endocytosis and potentiate EGFR signaling, stabilizing integrin α5ß1 adhesions may dampen EGFR signaling by slowing EGFR endocytosis. This notion resonates with the important earlier finding that certain cytoskeletal proteins such as Mena interact with integrin α5ß1 in a way that affects FAK activity and consequent downstream signaling [48].

Foundational work on endocytic trafficking processes has shown the EGFR signaling differs between the plasma membrane and in endosomes [49–51]; but the specific mediators of these processes remain poorly understood. One could imagine that a detailed analysis of endocytic vesicles containing EGFR and integrin α5ß1 in the presence and absence of P4G11 could identify key protein mediators of this process. If integrin α5ß1 directly recruits these mediators as it is recycled, it could suggest that integrin α5ß1 and its recycling rate is itself a broad mediator of signaling downstream of EGFR and perhaps other RTKs. This raises a hypothesis, testable in future work, that modulating endocytic processes may alter the recruited mediators and consequently modify downstream signaling and phenotypic effects.

Another conceivable possibility is that rather than a direct interaction between RTKs and integrins with downstream results, the dampening phenotype of P4G11 could be mediated indirectly via GSK3. Of the various signaling mediators, GSK3 is the protein most covaried with the P4G11-mediated negative regulation of RTK signaling phenotype and its inhibition reverses aspects of P4G11-mediated dampening. These data are surprising, as GSK3 is most commonly known as a tumor suppressor that negatively regulates the Wnt pathway [35].

When Wnt is activated, GSK3 is phosphorylated on an inhibitory site and rendered unable to perform its tumor suppressive functions, including preventing b-catenin degradation. In the context of EGFR signaling, EGF addition to cells has been shown to increase GSK3 inhibitory phosphorylation, thus inhibiting the tumor suppressor [52, 53]. Coordinate stimulation of murine epithelial cells *in vivo* with EGF and the same GSK3 inhibitor we use, CHIR-99021, leads to loss of junctional E-Cadherin and a thinning of the F-actin layer [54]. Our data support this, and we find that treatment of CC and Caco-2 cells in vitro with CHIR-99021 is sufficient to induce a loss of polarity which is not rescued by P4G11 treatment. This experiment is complicated by the role of GSK3 in the Wnt pathway and thus cell polarity, so further studies are necessary to determine the steps between P4G11-mediated integrin a5 clustering and GSK3 activity to ascertain the specificity of the role of GSK3 downstream of integrin a5. However, our data are in line with work showing that integrin α5 can be immunoprecipitated with dephosphorylated GSK3, phosphatase PP2P, and scaffolding protein RACK1 and is necessary for dephosphorylation of the inhibitory Ser9 residue [55]. Because GSK3 has hundreds of reported substrates including Akt and the focal adhesion scaffolding protein FAK [36, 37], it could serve as a link through which integrin α5β1 could broadly modulate EGFR and other RTKs. Hence, although integrin α5ß1 has frequently been cast to have a detrimental role in oncology as tumor cells with high levels of integrin recycling have increased proliferation, metastasis and angiogenesis, its contributions may be influenced by adhesion dynamics. This offers a further hypothesis, that can be tested by examining effects of FAK-mediated signaling modulators.

ACKNOWLEDGMENT

FUNDING

SUPPLEMENTARY DATA

Supplementary data are available at *INTBIO Journal* online.

REFERENCES

1. Lemmon MA, Schlessinger J. Cell signaling by receptor tyrosine kinases. *Cell* 2010;**141**:1117–34. doi: 10.1016/j.cell.2010.06.011.
2. Schlessinger J. Receptor tyrosine kinases: Legacy of the first two decades. *Cold Spring Harb Perspect Biol* 2014;**6**:a008912. doi: 10.1101/cshperspect.a008912.
3. Appert-Collin A, Hubert P, Crémel G et al Role of ErbB receptors in cancer cell migration and invasion. *Front Pharmacol* 2015;**6**:283. doi: 10.3389/fphar.2015.00283.

4. Aronheim A, Engelberg D, Li N et al Membrane targeting of the nucleotide exchange factor Sos is sufficient for activating the Ras signaling pathway. *Cell* 1994;**78**:949–61. doi: 10.1016/0092-8674(94)90271-2.

5. Rodrigues GA, Falasca M, Zhang Z et al A novel positive feedback loop mediated by the docking protein Gab1 and phosphatidylinositol 3-kinase in epidermal growth factor receptor signaling. *Mol Cell Biol* 2000;**20**:1448–59. doi: 10.1128/mcb.20.4.1448-1459.2000.

6. Sigismund S, Avanzato D, Lanzetti L. Emerging functions of the EGFR in cancer. *Mol Oncol* 2018;**12**:3–20. doi: 10.1002/1878-0261.12155.

7. Di Renzo MF, Olivero M, Giacomini A et al Overexpression and amplification of the met/HGF receptor gene during the progression of colorectal cancer. *Clin Cancer Res* 1995;**1**:147–54.

8. Joosten SPJ, Zeilstra J, van Andel H et al MET signaling mediates intestinal crypt-villus development, regeneration, and adenoma formation and is promoted by stem cell CD44 isoforms. *Gastroenterology* 2017;**153**:1040–53. doi: 10.1053/j.gastro.2017.07.008.

9. Roberts RB, Min L, Washington MK et al Importance of epidermal growth factor receptor signaling in establishment of adenomas and maintenance of carcinomas during intestinal tumorigenesis. *Proc Natl Acad Sci USA* 2002;**99**:1521–6. doi: 10.1073/pnas.032678499.

10. Katz M, Amit I, Yarden Y. Regulation of MAPKs by growth factors and receptor tyrosine kinases. *Biochim Biophys Acta* 2007;**1773**:1161–76. doi: 10.1016/j.bbamcr.2007.01.002.

11. Carey SP, Kraning-Rush CM, Williams RM et al Biophysical control of invasive tumor cell behavior by extracellular matrix microarchitecture. *Biomaterials* 2012;**33**:4157–65. doi: 10.1016/j.biomaterials.2012.02.029.

12. Cox BD, Natarajan M, Stettner MR et al New concepts regarding focal adhesion kinase promotion of cell migration and proliferation. *J Cell Biochem* 2006;**99**:35–52. doi: 10.1002/jcb.20956.

13. Hynes RO. The extracellular matrix: Not just pretty fibrils. *Science* 2009;**326**:1216–9. doi: 10.1126/science.1176009.

14. Chen Z, Oh D, Dubey AK et al EGFR family and Src family kinase interactions: Mechanics matters? *Curr Opin Cell Biol* 2018;**51**:97–102. doi: 10.1016/j.ceb.2017.12.003.

15. Morello V, Cabodi S, Sigismund S et al B1 integrin controls EGFR signaling and tumorigenic properties of lung cancer cells. *Oncogene* 2011;**30**:4087–96. doi: 10.1038/onc.2011.107.

16. Ning Y, Buranda T, Hudson LG. Activated epidermal growth factor receptor induces integrin α2 internalization via caveolae/raft-dependent endocytic pathway. *J Biol Chem* 2007;**282**:6380–6. doi: 10.1074/jbc.M610915200.

17. Wang F, Weaver VM, Petersen OW et al Reciprocal interactions between β1-integrin and epidermal growth factor receptor in three-dimensional basement membrane breast cultures: A different perspective in epithelial biology. *Proc Natl Acad Sci USA* 1998;**95**:14821–6. doi: 10.1073/pnas.95.25.14821.

18. Hang Q, Isaji T, Hou S et al Integrin α5 suppresses the phosphorylation of epidermal growth factor receptor and its cellular signaling of cell proliferation via N-glycosylation. *J Biol Chem* 2015;**290**:29345–60. doi: 10.1074/jbc.M115.682229.

19. Hang Q, Isaji T, Hou S et al N-glycosylation of integrin α5 acts as a switch for EGFR-mediated complex formation of integrin α5β1 to α6β4. *Sci Rep* 2016;**6**:33507. doi: 10.1038/srep33507.

20. Leabu M, Uniyal S, Xie J et al Integrin α2β1 modulates EGF stimulation of rho GTPase-dependent morphological changes in adherent human rhabdomyosarcoma RD cells. *J Cell Physiol* 2005;**202**:754–66. doi: 10.1002/jcp.20163.

21. Kuwada SK, Li X. Integrin α5/β1 mediates fibronectin-dependent epithelial cell proliferation through epidermal growth factor receptor activation. *Mol Biol Cell* 2000;**11**:2485–96. doi: 10.1091/mbc.11.7.2485.

22. Lee JW, Juliano RL. The α5β1 integrin selectively enhances epidermal growth factor signaling to the phosphatidylinositol-3-kinase/Akt pathway in intestinal epithelial cells. *Biochim Biophys Acta* 2002;**1542**:23–31. doi: 10.1016/S0167-4889(01)00161-6.

23. Lee JW, Juliano RL. α5β1 integrin protects intestinal epithelial cells from apoptosis through a phosphatidylinositol 3-kinase and protein kinase B-dependent pathway. *Mol Biol Cell* 2000;**11**(6):1973–87. doi: 10.1091/mbc.11.6.1973.

24. Varner JA, Emerson DA, Juliano RL. Integrin α5β1 expression negatively regulates cell growth: Reversal by attachment to fibronectin. *Mol Biol Cell* 1995;**6**:725–40. doi: 10.1091/mbc.6.6.725.

25. Starchenko A, Graves-Deal R, Yang Y-P et al Clustering of integrin α5 at the lateral membrane restores epithelial polarity in invasive colorectal cancer cells. *Mol Biol Cell* 2017;**28**:1288–300. doi: 10.1091/mbc.E16-12-0852.

26. Schäfer J, Strimmer K. An empirical Bayes approach to inferring large-scale gene association networks. *Bioinformatics* 2005;**21**:754–64. doi: 10.1093/bioinformatics/bti062.

27. Xue Q, Lu Y, Eisele MR et al Analysis of single-cell cytokine secretion reveals a role for paracrine signaling in coordinating macrophage responses to TLR4 stimulation. *Sci Signal* 2015;**8**:ra59. doi: 10.1126/scisignal.aaa2155.

28. Ivaska J, Heino J. Cooperation between integrins and growth factor receptors in signaling and endocytosis. *Annu Rev Cell Dev Biol* 2011;**27**:291–320. doi: 10.1146/annurev-cell-bio-092910-154017.

29. Li C, Singh B, Graves-Deal R et al Three-dimensional culture system identifies a new mode of cetuximab resistance and disease-relevant genes in colorectal cancer. *Proc Natl Acad Sci USA* 2017;**114**:E2852–61. doi: 10.1073/pnas.1618297114.

30. Campbell ID, Humphries MJ. Integrin structure, activation, and interactions. *Cold Spring Harb Perspect Biol* 2011;**3**:a004994. doi: 10.1101/cshperspect.a004994.

31. Mould AP, Askari JA, Byron A et al Ligand-induced epitope masking: Dissociation of integrin α5β1-fibronectin complexes only by monoclonal antibodies with an allosteric mode of action. *J Biol Chem* 2016;**291**:20993–1007. doi: 10.1074/jbc.M116.736942.

32. Mould AP, Garratt AN, Puzon-McLaughlin W et al Regulation of integrin function: Evidence that bivalent-cation-induced conformational changes lead to the unmasking of ligand-binding sites within integrin α5β1. *Biochem J* 1998;**331**:821–8. doi: 10.1042/bj3310821.

33. Lau KS, Juchheim AM, Cavaliere KR et al In vivo systems analysis identifies spatial and temporal aspects of the modulation of TNFa-induced apoptosis and proliferation by MAPKs. *Sci Signal* 2011;**4**:ra16–6. doi: 10.1126/scisignal.2001338.

34. McCubrey JA, Steelman LS, Bertrand FE et al GSK-3 as potential target for therapeutic intervention in cancer. *Oncotarget* 2014;**5**:2881–911. doi: 10.18632/oncotarget.2037.

35. Beurel E, Grieco SF, Jope RS. Glycogen synthase kinase-3 (GSK3): Regulation, actions, and diseases. *Pharmacol Ther* 2015;**148**:114–31. doi: 10.1016/j.pharmthera.2014.11.016.

36. Hermida MA, Dinesh Kumar J, Leslie NR. GSK3 and its interactions with the PI3K/AKT/mTOR signalling network. *Adv Biol Regul* 2017;**65**:5–15. doi: 10.1016/j.jbior.2017.06.003.

37. Bianchi M, De Lucchini S, Marin O et al Regulation of FAK Ser-722 phosphorylation and kinase activity by GSK3 and PP1 during cell spreading and migration. *Biochem J* 2005;**391**:359–70. doi: 10.1042/BJ20050282.

38. Severson EA, Kwon M, Hilgarth RS et al Glycogen synthase kinase 3 (GSK-3) influences epithelial barrier function by regulating Occludin, Claudin-1 and E-cadherin expression. *Biochem Biophys Res Commun* 2010;**397**:592. doi: 10.1016/J.BBRC.2010.05.164.

39. Bennett CN, Ross SE, Longo KA et al Regulation of Wnt signaling during adipogenesis. *J Biol Chem* 2002;**277**:30998–1004. doi: 10.1074/jbc.M204527200.

40. Kim, H.D., Meyer, A.S., Wagner, J.P., Alford, S.K., Wells, A., Gertler, F.B., &Lauffenburger, D.A. (2011). Signaling network state predicts twist-mediated effects on breast cell migration across diverse growth factor contexts. *Mol Cell Proteomics,* **10**: M111.008433. https//doi.org/10.1074/mcp.M111.008433

41. Jones DS, Jenney AP, Joughin BA et al Inflammatory but not mitogenic contexts prime synovial fibroblasts for compensatory signaling responses to p38 inhibition. *Sci Signal* 2018;**11**:eaa1601. doi: 10.1126/scisignal.aal1601.

42. Kanda R, Kawahara A, Watari K et al Erlotinib resistance in lung cancer cells mediated by integrin beta1/Src/Akt-driven bypass signaling. *Cancer Res* 2013;**73**:6243–353. doi: 10.1158/0008-5472.CAN-12-4502.

43. Kim, S., Kang, H.Y., Nam, E.H., Choi, M.S., Zhao, X.F., Hong, C.S., Lee, J.W., Lee, J.H., & Park, Y.K. (2010). TMPRSS4 induces invasion and epithelial-mesenchymal transition through upregulation of integrin alpha5 and its signaling pathways. *Carcinogenesis,* **31**: 597–606. https//doi.org/10.1093/carcin/bgq024

44. Wang M, Zhang G, Zhang Y et al Fibrinogen alpha chain knockout promotes tumor growth and metastasis through integrin-Akt signaling pathway in lung cancer. *Mol Cancer Res* 2020;**18**:943–54. doi: 10.1158/1541-7786.MCR-19-1033.

45. Krishnan M, Lapierre LA, Knowles BC et al Rab25 regulates integrin expression in polarized colonic epithelial cells. *Mol Biol Cell* 2013;**24**:818–31. doi: 10.1091/mbc.E12-10-0745.

46. Lapierre LA, Caldwell CM, Higginbotham JN et al Transformation of rat intestinal epithelial cells by overexpression of Rab25 is microtubule dependent. *Cytoskeleton* 2011;**68**:97–111. doi: 10.1002/cm.20497.

47. Jeong H, Lim KM, Kim KH et al Loss of Rab25 promotes the development of skin squamous cell carcinoma through the dysregulation of integrin trafficking. *J Pathol* 2019;**249**:227–40. doi: 10.1002/path.5311.

48. Gupton SL, Riquelme D, Hughes-Alford SK et al Mena binds α5 integrin directly and modulates α5β1 function. *J Cell Biol* 2012;**198**:657–76. doi: 10.1083/jcb.201202079.

49. Goh LK, Sorkin A. Endocytosis of receptor tyrosine kinases. *Cold Spring Harb Perspect Med* 2013;**5**:a017459. doi: 10.1007/978-0-387-39951-5_9.

50. Vieira AV, Lamaze C, Schmid SL. Control of EGF receptor signaling by clathrin-mediated endocytosis. *Science* 1996;**274**:2086–9. doi: 10.1126/science.274.5295.2086.

51. Wiley HS, Burke PM. Regulation of receptor tyrosine kinase signaling by endocytic trafficking. *Traffic* 2001;12–8. doi: 10.1034/j.1600-0854.2001.020103.x.

52. Eldar-Finkelman H, Seger R, Vandenheede JR et al Inactivation of glycogen synthase kinase-3 by epidermal growth factor is mediated by mitogen-activated protein kinase/p90 ribosomal protein S6 kinase signaling pathway in NIH/3T3 cells. *J Biol Chem* 1995;**270**:987–90. doi: 10.1074/JBC.270.3.987.

53. Saito Y, Vandenheede JR, Cohen P. The mechanism by which epidermal growth factor inhibits glycogen synthase kinase 3 in A431 cells. *Biochem J* 1994;**303**:27–31. http://www.ncbi.nlm.nih.gov/pubmed/7945252.

54. Kozlowski MM, Rudolf MA, Corwin JT. EGF and a GSK3 inhibitor deplete junctional e-cadherin and stimulate proliferation in the mature mammalian ear. *J Neurosci* 2020;**40**:2618–32. doi: 10.1523/JNEUROSCI.2630-19.2020.

55. De Toni-Costes F, Despeaux M, Bertrand J et al A new α5β1 integrin-dependent survival pathway through GSK3β activation in leukemic cells. *PLoS ONE* 2010;**5**:e9807. doi: 10.1371/journal.pone.0009807.